A&A 442, L25–L29 (2005)
DOI: 10.1051/0004-6361:200500180

Astronomy & Astrophysics

A possible association of the new VHE γ-ray source HESS J1825–137 with the pulsar wind nebula G 18.0–0.7

F. A. Aharonian[1], A. G. Akhperjanian[2], A. R. Bazer-Bachi[3], M. Beilicke[4], W. Benbow[1], D. Berge[1], K. Bernlöhr[1,5], C. Boisson[6], O. Bolz[1], V. Borrel[3], I. Braun[1], F. Breitling[5], A. M. Brown[7], P. M. Chadwick[7], L.-M. Chounet[8], R. Cornils[4], L. Costamante[1,20], B. Degrange[8], H. J. Dickinson[7], A. Djannati-Ataï[9], L. O'C. Drury[10], G. Dubus[8], D. Emmanoulopoulos[11], P. Espigat[9], F. Feinstein[12], G. Fontaine[8], Y. Fuchs[13], S. Funk[1], Y. A. Gallant[12], B. Giebels[8], S. Gillessen[1], J. F. Glicenstein[14], P. Goret[14], C. Hadjichristidis[7], M. Hauser[11], G. Heinzelmann[4], G. Henri[13], G. Hermann[1], J. A. Hinton[1], W. Hofmann[1], M. Holleran[15], D. Horns[1], A. Jacholkowska[12], O. C. de Jager[15], B. Khélifi[1], Nu. Komin[5], A. Konopelko[1,5], I. J. Latham[7], R. Le Gallou[7], A. Lemière[9], M. Lemoine-Goumard[8], N. Leroy[8], T. Lohse[5], J. M. Martin[6], O. Martineau-Huynh[16], A. Marcowith[3], C. Masterson[1,20], T. J. L. McComb[7], M. de Naurois[16], S. J. Nolan[7], A. Noutsos[7], K. J. Orford[7], J. L. Osborne[7], M. Ouchrif[16,20], M. Panter[1], G. Pelletier[13], S. Pita[9], G. Pühlhofer[1,11], M. Punch[9], B. C. Raubenheimer[15], M. Raue[4], J. Raux[16], S. M. Rayner[7], A. Reimer[17], O. Reimer[17], J. Ripken[4], L. Rob[18], L. Rolland[16], G. Rowell[1], V. Sahakian[2], L. Saugé[13], S. Schlenker[5], R. Schlickeiser[17], C. Schuster[17], U. Schwanke[5], M. Siewert[17], H. Sol[6], D. Spangler[7], R. Steenkamp[19], C. Stegmann[5], J.-P. Tavernet[16], R. Terrier[9], C. G. Théoret[9], M. Tluczykont[8,20], G. Vasileiadis[12], C. Venter[15], P. Vincent[16], H. J. Völk[1], and S. J. Wagner[11]

[1] Max-Planck-Institut für Kernphysik, Heidelberg, Germany [2] Yerevan Physics Institute, Yerevan, Armenia [3] Centre d'Étude Spatiale des Rayonnements, CNRS/UPS, Toulouse, France [4] Universität Hamburg, Institut für Experimentalphysik, Hamburg, Germany [5] Institut für Physik, Humboldt-Universität zu Berlin, Germany [6] LUTH, UMR 8102 du CNRS, Observatoire de Paris, Section de Meudon, France [7] University of Durham, Department of Physics, Durham DH1 3LE, UK [8] Laboratoire Leprince-Ringuet, IN2P3/CNRS, Ecole Polytechnique, Palaiseau, France [9] APC, Paris Cedex 05, France⋆ [10] Dublin Institute for Advanced Studies, Dublin, Ireland [11] Landessternwarte, Königstuhl, Heidelberg, Germany [12] Laboratoire de Physique Théorique et Astroparticules, Université Montpellier II, France [13] Laboratoire d'Astrophysique de Grenoble, INSU/CNRS, Université Joseph Fourier, France [14] DAPNIA/DSM/CEA, CE Saclay, Gif-sur-Yvette, France [15] Unit for Space Physics, North-West University, Potchefstroom, South Africa, e-mail: fskocdj@puk.ac.za [16] Laboratoire de Physique Nucléaire et de Hautes Énergies, IN2P3/CNRS, Universités Paris VI & VII, France [17] Institut für Theoretische Physik, Lehrstuhl IV, Ruhr-Universität Bochum, Germany [18] Institute of Particle and Nuclear Physics, Charles University, Prague, Czech Republic [19] University of Namibia, Windhoek, Namibia [20] European Associated Laboratory for Gamma-Ray Astronomy, jointly supported by CNRS and MPG

Received 27 July 2005 / Accepted 3 September 2005

ABSTRACT

We report on a possible association of the recently discovered very high-energy γ-ray source HESS J1825–137 with the pulsar wind nebula (commonly referred to as G 18.0–0.7) of the 2.1×10^4 year old Vela-like pulsar PSR B1823–13. HESS J1825–137 was detected with a significance of 8.1σ in the Galactic Plane survey conducted with the HESS instrument in 2004. The centroid position of HESS J1825–137 is offset by 11′ south of the pulsar position. *XMM-Newton* observations have revealed X-ray synchrotron emission of an asymmetric pulsar wind nebula extending to the south of the pulsar. We argue that the observed morphology and TeV spectral index suggest that HESS J1825–137 and G 18.0–0.7 may be associated: the lifetime of TeV emitting electrons is expected to be longer compared to the *XMM-Newton* X-ray emitting electrons, resulting in electrons from earlier epochs (when the spin-down power was larger) contributing to the present TeV flux. These electrons are expected to be synchrotron cooled, which explains the observed photon index of ∼2.4, and the longer lifetime of TeV emitting electrons naturally explains why the TeV nebula is larger than the X-ray size. Finally, supernova remnant expansion into an inhomogeneous medium is expected to create reverse shocks interacting at different times with the pulsar wind nebula, resulting in the offset X-ray and TeV γ-ray morphology.

Key words. ISM: plerions – ISM: individual objects: PSR B1823–13, HESS J1825–137, G 18.0–0.7 – gamma-rays: observations

⋆ UMR 7164 (CNRS, Observatoire de Paris).

1. Introduction

PSR B1823–13 (also known as PSR J1826–1334) is a 101 ms evolved pulsar with a spin-down age of $T = 2.1 \times 10^4$ years (Clifton et al. 1992) and in these properties very similar to the Vela pulsar. It is located at a distance of $d = 3.9 \pm 0.4$ kpc (Cordes & Lazio 2002) and *ROSAT* observations of this source with limited photon statistics revealed a compact core, as well as an extended diffuse nebula of size ∼5′ south-west of the pulsar (Finley et al. 1998). High resolution *XMM-Newton* observations of the pulsar region confirmed this asymmetric shape and size of the diffuse nebula, which was hence given the name G 18.0–0.7 (Gaensler et al. 2003). For the compact core with extent $R_{\rm CN} \sim 30''$ (CN: compact nebula) immediately surrounding the pulsar, a photon index of $\Gamma_{\rm CN} = 1.6^{+0.1}_{-0.2}$ was measured with a luminosity of $L_{\rm CN} \sim 9 d_4^2 \times 10^{32}$ erg s^{-1} in the 0.5 to 10 keV range for a distance of $4d_4$ kpc. The corresponding pulsar wind shock radius is $R_{\rm s} \leq 15'' = 0.3 d_4$ pc. The compact core is embedded in a region of extended diffuse emission which is clearly one-sided, revealing a structure south of the pulsar, with an extension of $R_{\rm EN} \sim 5'$, (EN: extended nebula) whereas the ∼4′ east-west extension is symmetric around the north-south axis. The spectrum of this extended component is softer with a photon index of $\Gamma_{\rm EN} \sim 2.3$, with a luminosity of $L_{\rm EN} = 3 d_4^2 \times 10^{33}$ erg s^{-1} for the 0.5 to 10 keV interval. No associated supernova remnant (SNR) has been identified yet.

At γ-ray energies, PSR B1823–13 was proposed to power the close-by unidentified EGRET source 3EG J1826−1302 (Nolan et al. 2003). TeV observations of this pulsar by the Whipple and HEGRA Collaborations resulted in only upper limits (Hall et al. 2003; Aharonian et al. 2002), which are unconstraining with respect to HESS.

The region around PSR B1823–13 was observed as part of the survey of the Galactic plane with the HESS instrument (Aharonian et al. 2005a). In this survey, a source of very high-energy (VHE) γ-rays (HESS J1825–137) 11′ south of the pulsar was discovered with a significance of 8.1σ. We note that the new VHE γ-ray source is located within the 95% positional confidence level of the EGRET source 3EG J1826–1302 and could therefore be related to this as of yet unidentified object. The High Energy Stereoscopic System (HESS) is an array of four imaging atmospheric Cherenkov telescopes located in the Khomas Highland of Namibia (Hinton 2004). It is designed for the observation of astrophysical sources in the energy range from 100 GeV to several tens of TeV. The system was completed in December 2003 and has already provided a number of significant detections of galactic γ-ray sources. These include the first detection of spatially extended emission from a pulsar wind nebula (PWN) in very high-energy γ-rays (Aharonian et al. 2005b). Each HESS telescope has a mirror area of 107 m^2 (Bernlöhr et al. 2003) and the system is run in a coincidence mode (Funk et al. 2004) requiring at least two of the four telescopes to have triggered in each event. The HESS instrument has an energy threshold of ≈100 GeV at zenith, an angular resolution of ∼0.1° per event and a point source sensitivity of <2.0× 10^{-13} cm^{-2} s^{-1} (1% of the flux from the Crab Nebula) for a 5σ detection in a 25 h observation.

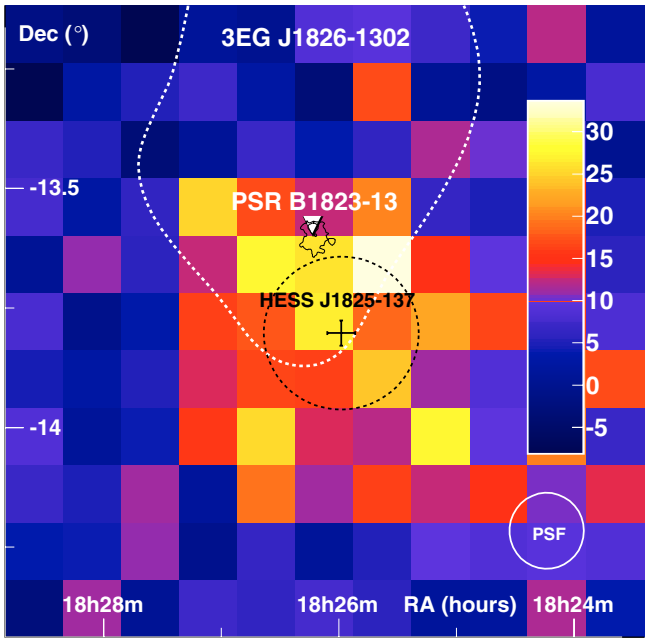

Fig. 1. Excess map of the region close to PSR B1823–13 (marked with a triangle) with uncorrelated bins. The best fit centroid of the γ-ray excess is shown with error bars. The black dotted circle shows the best fit emission region size ($\sigma_{\rm source}$) assuming a Gaussian brightness profile. The black contours denote the X-ray emission as detected by *XMM-Newton*. The 95% confidence region (dotted white line) for the position of the unidentified EGRET source 3EG J1826–1302 is also shown. The system acceptance is uniform at the 20% level in a 0.6° radius circle around HESS J1825–137.

2. HESS observations and results

The first HESS observations of this region occurred as part of a systematic survey of the inner Galaxy from May to July 2004 (with 4.2 h of exposure within 2° of HESS J1825−137). Evidence for a VHE γ-ray signal in these data triggered re-observations from August to September 2004 (5.1 h). The mean zenith angle of the observations was 31° and the mean offset (ψ) of the source from the pointing direction of the system was 0.9°. The off-axis sensitivity of the system derived from Monte-Carlo simulations has been confirmed via observations of the Crab Nebula (Aharonian et al. 2005c). The data set corresponds to a total live-time of 8.4 h after application of run quality selection based on weather and hardware conditions.

The standard scheme for the reconstruction of events was applied to the data (see Aharonian et al. 2005d for details). Cuts on the scaled width and length of images (optimized on γ-ray simulations and off-source data) were used to suppress the hadronic background. While in the standard scheme an image size cut of 80 photoelectrons (pe) was used to ensure well reconstructed images, in the search for weak sources an additional image size cut of 200 pe was applied to achieve optimum sensitivity. This cut reduces the background by a factor of 7 at the expense of an increased analysis threshold of 420 GeV. A model of the field of view acceptance, derived from off-source runs, is used to estimate the background. Figure 1 shows an uncorrelated excess count map of the 1.6° × 1.6° region around HESS J1825–137. A clear and extended excess is observed to

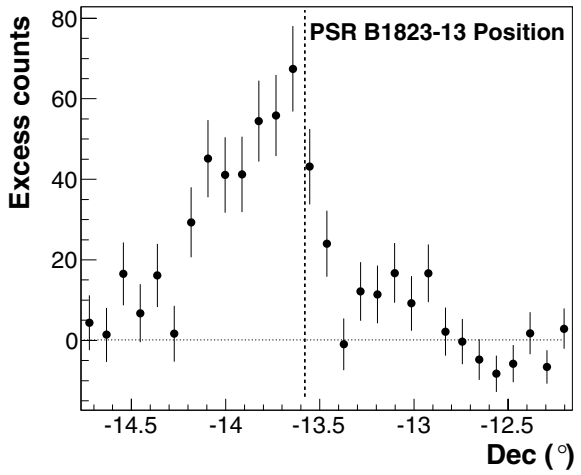

Fig. 2. Acceptance-corrected excess slice through the region surrounding HESS J1825–137 along the north-south direction of width 0.4°. The pulsar position is marked with a dotted line. The one-sided nature of the emission with a slow decline to the south of the pulsar is evident.

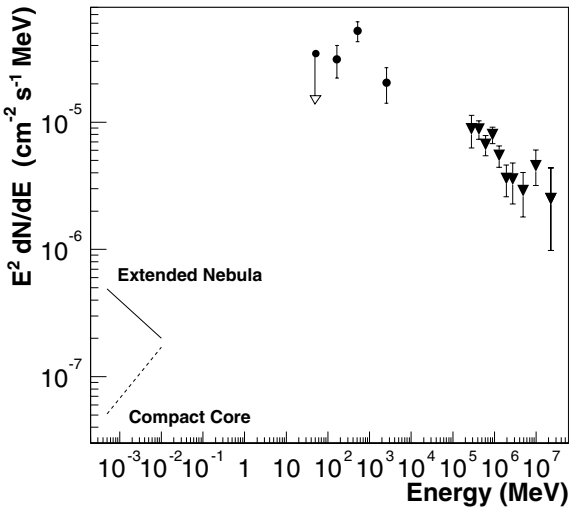

Fig. 3. Spectral energy distribution of HESS J1825–137, assuming that the X-ray emission surrounding PSR B1823–13, the EGRET source 3EG J1826–1302 and the new VHE γ-ray source are related. X-ray data, indicated by lines, are taken from Gaensler et al. (2003) and are shown for the two different regions as described in the text. EGRET data (full circles) are taken from the third EGRET catalog (Hartman et al. 1999). The triangles show the HESS data from this work.

the south of the pulsar PSR B1823–13. Assuming a radially symmetric Gaussian brightness profile ($\rho \propto \exp(-\theta^2/2\sigma^2_{\rm source})$) an extension of $\sigma_{\rm source} = 9.6' \pm 2.0'$ is derived. The best fit position for the centre of the excess lies at a distance of 11.2′ from PSR B1823–13 at 18h26m3s±7s, −13°45.7′±1.7′. On the scale of the measured displacement the systematic HESS pointing uncertainties of 20″ are negligible. Figure 2 shows an acceptance corrected excess slice through the region surrounding HESS J1825–137, in the north-south direction, of width 0.4°. The position of PSR B1823–13 is marked with a dotted line. It can be seen that the VHE emission extends asymmetrically to the south of the pulsar. Using the best-fit position we derive a statistical significance of 8.1σ after accounting for all trials involved in the search for sources (Aharonian et al. 2005a). This significance is obtained counting events within a circle of radius $\theta = 0.22°$ ($\theta^2 = 0.05$ deg^2), a value chosen a priori for the search for extended sources (Aharonian et al. 2005a). Using a larger angular cut appropriate to contain the complete emission region of HESS J1825–137 of $\theta = 0.4°$ an excess of 370 ± 20 and a statistical significance of 13.4σ are derived.

For spectral analysis, the looser image size cut of 80 pe and the wide angular cut of $\theta < 0.4°$ are applied to extend the source spectrum to lower energies (resulting in a threshold of 230 GeV). To reduce systematic errors, only runs with $\psi < 1.5°$ offset from the on-region are used, resulting in a total live-time of 5.4 h. The background is estimated from regions with equal offset ψ from the centre of the field of view, again to minimize systematic errors. The derived spectral energy distribution is shown in Fig. 3. The HESS spectrum can be fitted by a power law in energy with photon index $2.40 \pm 0.09_{\rm stat} \pm 0.2_{\rm sys}$ and a flux above 230 GeV of $(3.4 \pm 0.2_{\rm stat} \pm 1.0_{\rm sys}) \times 10^{-11}$ cm^{-2} s^{-1} (corresponding to 12% of the Crab flux above that energy). The fit has a χ^2/d.o.f. of 9.8/8. A spectral analysis using a 200 pe image cut yields consistent results. We estimate the systematic error on the absolute flux level to be 30%. We find no evidence for intra-night variability of the γ-ray flux. A fit of the night-by-night γ-ray flux of the source to a constant value yields a χ^2/d.o.f. of 9.2/7.

3. The association of HESS J1825–137 with G 18.0–0.7

HESS J1825–137 was discovered during an unbiased survey of the galactic plane within the central ±30° longitude sector. Multiwavelength searches within a circle of radius $\sigma_{\rm source} \sim 10'$ around the centre of gravity revealed PSR B1823–13, at the edge of the source radius, as the only plausible candidate counterpart. The discussion below investigates the possibility of associating the pulsar and its nebula G18.0–0.7 with HESS J1825–137.

The one-sided nature of this PWN as seen in TeV was already suggested by Gaensler et al. (2003), for the X-rays, based on the hydrodynamical simulations of Blondin et al. (2001) for Vela X and earlier studies referenced by Gaensler et al.: it was assumed that the density of the medium surrounding the progenitor star was inhomogeneous along the north-south direction, with the density towards the northern direction significantly larger than to the south. The reverse shock from the northern direction should then have crashed relatively early into the PWN, pushing the latter towards the south, as observed. The apparent diameter ∼0.5° of the TeV source indicates a relatively large PWN size, $R_{\rm PWN} = 17 d_4$ pc. The unseen SNR shell in this scenario would have to be substantially larger: in the simulations of Blondin et al. (2001), as well as in a sample of observed composite SNRs (van der Swaluw & Wu 2001), the ratio $R_{\rm PWN}/R_{\rm SNR}$ does not exceed ∼0.25. The large implied $R_{\rm SNR}$ would suggest that the blast wave is expanding into a low-density medium to the south. For instance, a remnant in the Sedov-Taylor phase expanding into the hot phase

of the interstellar medium, with density ~ 0.003 cm^{-3}, would have $R_{\rm SNR} = 58$ pc at $T = 21.5$ kyears (assuming an explosion energy of 10^{51} erg). This is somewhat smaller than the value implied by the size of the TeV source, but uncertainties in the distance estimate should be kept in mind, as well as the fact that with a braking index different from 3 (as discussed below), the true pulsar age might be greater than the nominal spin-down time. Within the scenario outlined above, a high initial spin-down luminosity, or the fact that the SNR reverse shock on the southern side might not yet have reached the PWN, could also yield a larger value for $R_{\rm PWN}/R_{\rm SNR}$ (Bucciantini et al. 2004, and references therein). Finally, the accelerated electrons might diffuse beyond the boundary of the PWN, where they would still radiate by the inverse Compton mechanism but emit little synchrotron radiation (Aharonian et al. 1997), making the TeV source extension larger than otherwise be expected.

The synchrotron lifetime of VHE electrons in a field of strength $B = 10^{-5}B_{-5}$ G, scattering cosmic microwave background (CMBR) photons to energies $E_\gamma = 10^{12}E_{\rm TeV}$ eV (in the Thomson limit) can be shown to be $\tau(E_\gamma) = 4.8B_{-5}^{-2}E_{\rm TeV}^{-1/2}$ kyears, whereas the corresponding lifetime of keV emitting electrons is shorter: $\tau(E_{\rm X}) = 1.2B_{-5}^{-3/2}E_{\rm keV}^{-1/2}$ kyears, where $E_{\rm keV}$ is the synchrotron photon energy in units of keV. Gaensler et al. have argued that the field strength in the extended X-ray nebula is ~ 10 μG, so that we assume $B_{-5} = 1$ for the X-ray and TeV emitting zones. The adiabatic loss and escape time scales from the compact nebula are a few years; this is much shorter than the corresponding synchrotron lifetime of X-ray emitting electrons, given typical values of Vela-like compact nebular field strengths. Synchrotron losses in the compact nebula therefore do not modify the electron spectral index of ~ 2.2 in this region, which is responsible for the observed compact nebular photon index of $\Gamma_{\rm CN} \sim 1.6$ in the 0.5 to 10 keV range. The shocked pulsar wind particles in the offset nebula will then propagate southwards until the propagation time is equal to the synchrotron loss time, which will result in a steepening in the X-ray photon index to the observed value of $\Gamma_{\rm EN} \sim 2.3$. If V_γ and $V_{\rm X}$ are the average wind convection speeds corresponding to the respective γ-ray and X-ray emitting zones, the ratio between the predicted TeV and X-ray sizes should then be $R_\gamma/R_{\rm X} = 4(V_\gamma/V_{\rm X})B_{-5}^{-1/2}(\overline{E}_{\rm keV}/\overline{E}_{\rm TeV})^{1/2}$, which can easily predict a TeV nebula which is ~ 6 times larger than the X-ray nebula, given the respective experimental mean X-ray and γ-ray photon energies of $\overline{E}_{\rm keV} \sim 2$ (after absorption) and $\overline{E}_{\rm TeV} \sim 0.9$. This ratio (of six) also assumes that the expansion velocity of the PWN does not change significantly between the extended X-ray and TeV nebulae (i.e. $V_\gamma \sim V_{\rm X}$). It should however be noted that this is a naive assumption and that a detailed study of the evolution of the velocity and associated magnetic field distributions should be made.

Pulsars spin down with a braking law given by $\dot{\Omega} = -K\Omega^n$, where Ω is the spin angular frequency and K is a constant, depending on the surface magnetic field strength and neutron star equation of state. Assuming typical pulsar braking indices $n \sim 2.5$ to 3, we can integrate over the spindown power $\dot{E}$ (assuming a conversion efficiency of $\sim 50\%$ to electrons) to an epoch $\tau(E_\gamma)$ into the past when $\dot{E}$ was larger, to give the total electron spectrum contributing to the HESS spectral band (from 0.23 TeV to >10 TeV). Since we integrate over the past $\tau_{\rm max} \sim 9B_{-5}^{-2}$ kyears (corresponding to a minimum energy of 0.23 TeV), which represents $\sim 50\%$ of the pulsar lifetime, uncertainties in n should still be relatively unimportant. The total observed TeV spectrum is then the result of a summation of successive inverse Compton spectra arising from past injected electron spectra, with the spectral break energy shifting down with time T into the past as T^{-2}. The result is a cooled TeV spectrum, for which the TeV γ-ray photon index $\Gamma_{\rm TeV}$ should be larger than $\Gamma_{\rm CN} + 0.5 \sim 2.1$ due to second-order Klein-Nishina effects on the production spectrum of IC radiation on the CMBR. A detailed discussion of this is beyond the scope of this paper, but the important point is that the observed TeV photon index in the range 2.2 to 2.6 is consistent with this interpretation. Furthermore, because the TeV emission is the result of earlier epochs of pulsar injection, the ratio of γ-ray luminosity to present spin-down power would over-estimate the true conversion efficiency. Compare the X-ray and γ-ray energy fluxes in Fig. 3: the TeV energy flux is larger than the X-ray energy fluxes, with the latter resulting from more freshly injected electrons.

EGRET did not detect pulsed emission above 100 MeV from this pulsar (Nel et al. 1996) and phase-resolved spectroscopy is required to set upper limits on the pulsed component associated with PSR B1823–13, to see if this component is significantly lower than the EGRET steady excess shown in Fig. 3. If 3EG J1826–1302 is also associated with G 18.0–0.7, the GeV emitting electrons would represent the earliest epochs of pulsar injection. This emission should also be one-sided within the framework discussed above and future GLAST observations may be able to provide better constraints on the GeV morphology.

Acknowledgements. The support of the Namibian authorities and of the University of Namibia in facilitating the construction and operation of HESS is gratefully acknowledged, as is the support by the German Ministry for Education and Research (BMBF), the Max Planck Society, the French Ministry for Research, the CNRS-IN2P3 and the Astroparticle Interdisciplinary Programme of the CNRS, the UK Particle Physics and Astronomy Research Council (PPARC), the IPNP of the Charles University, the South African Department of Science and Technology and National Research Foundation, and by the University of Namibia. We appreciate the excellent work of the technical support staff in Berlin, Durham, Hamburg, Heidelberg, Palaiseau, Paris, Saclay, and in Namibia in the construction and operation of the equipment.

References

Aharonian, F. A., Atoyan, A., & Kifune, T. 1997, MNRAS, 291, 162
Aharonian, F. A., Akhperjanian, A. G., Beilicke, M., et al. (HEGRA Collaboration) 2002, A&A, 395, 803
Aharonian, F. A., Akhperjanian, A. G., Aye, K.-M., et al. (HESS Collaboration) 2005a, Science, 307, 1938
Aharonian, F. A., Akhperjanian, A. G., Aye, K.-M., et al. (HESS Collaboration) 2005b, A&A, 435, L17

Aharonian, F. A., et al. (HESS Collaboration) 2005c, A&A, to be submitted
Aharonian, F. A., Akhperjanian, A. G., Aye, K.-M., et al. (HESS Collaboration) 2005d, A&A, 430, 865
Bernlöhr, K., et al. 2003, Astropart. Phys., 20, 111
Blondin, J. M., Chevalier, R. A., & Frierson, D. M. 2001, ApJ, 563, 806
Bucciantini, N., Bandiera, R., Blondin, J. M., Amato, E., & Del Zanna, L. 2004, A&A, 422, 609
Clifton, T. R., Lyne, A. G., Jones, A. W., McKenna, J., & Ashworth, M. 1992, MNRAS, 254, 177
Cordes, J. M., & Lazio, T. J. W. 2002, preprint [arXiv:astro-ph/0207156]
Finley, J. P., Srinivasan, R., & Park, S. 1996, 466, 938
Funk, S., Hermann, G., Hinton, J., et al. 2004, Astropart. Phys., 22, 285
Gaensler, B. M., Schulz, N. S., Kaspi, V. M., Pivovaroff, M. J., & Becker, W. E. 2003, ApJ, 588, 441
Hall, T. A., et al. 2003, Proc. 28th ICRC, Tsukuba, Univ. Academy Press, Tokyo, 2497
Hartman, R. C., Bertsch, D. L., Bloom, S. D., et al. 1999, ApJS, 123, 79
Hinton, J. A. (HESS Collaboration) 2004, New Astron. Rev., 48, 331
Nel, H. I., Arzoumanian, Z., Bailes, M., et al. 1996, ApJ, 465, 898
Nolan, P. L., Tompkins, W. F., Grenier, I. A., & Michelson, P. F. 2003, ApJ, 597, 615
van der Swaluw, E., & Wu, Y. 2001, ApJ, 555, L49